Complete spatial characterization of a pulsed doughnut-type beam by use of spherical optics and a cylindrical lens

Julio Serna and Fernando Encinas-Sanz

Departamento de Óptica, Facultad de Ciencias Físicas, Universidad Complutense, 28040 Madrid, Spain

George Nemeş

Astigmat, 1118 Starbird Circle, Suite 23, San Jose, California 95117

Received October 25, 2000; revised manuscript received January 22, 2001; accepted February 16, 2001

A complete spatial characterization (in second-order moments) of a doughnut-type beam from a pulsed transversely excited atmospheric CO_2 laser is described. It includes the measurement of the orbital angular momentum carried by the beam. The key element in the characterization is the use of a cylindrical lens in addition to the usual spherical optics. Internal features of the beam that would have remained hidden if only spherical optics were employed were revealed by use of the cylindrical lens. The experimental results are compared and agree with a theoretical Laguerre–Gauss mode beam. © 2001 Optical Society of America

OCIS codes: 140.3460, 140.3470.

1. INTRODUCTION

The spatial characterization of laser beams has become an important topic in itself. The beams produced by industrial and research lasers need to be well known and specified to permit useful and reproducible results to be obtained from their use. Along this line characterization based on the Wigner distribution function and on the irradiance second-order moments of beams has proven to be very useful.[1–6] Such characterization remains the basis of an International Organization for Standardization (ISO) standard,[7] although some limitations have been proposed and introduced in the scope of the standard.[7–9]

Within this formalism the most general three-dimensional beam is characterized completely if the ten elements of its beam matrix are known.[5] Nine of these elements (those related to the beam size, the beam divergence, and the radius of curvature) can be obtained from irradiance measurements by use of spherical lenses and free-propagation sections. But the tenth element, which is related to the orbital angular momentum that is transported by the beam,[6] remains hidden if only optical systems with rotational symmetry are used.[8] Several setups have been proposed for measuring all the elements of the beam matrix.[10,11] In these setups at least one cylindrical lens has to be used during measurement to reveal the information that is related to the orbital angular momentum. Otherwise, the characterization of the beam is only partial and could lead to errors.[8] Some experimental results have been obtained for pseudostigmatic beams[8,9] that are generated from simple astigmatic beams,[10] and they have been compared with the theoretical predictions.[11]

The purpose of this paper is to apply the theory of measuring pseudosymmetrical, or pseudotype, beams[8,9] to a beam that comes unmodified from a laser head and not to a specially conditioned beam, as was done in previous studies. To our knowledge, this study is among the first to present measurements to reveal the pseudosymmetrical behavior of a beam from a laser without special accommodations for inducing such behavior outside the laser cavity. Note that, without the cylindrical lens in the measurement, the pseudosymmetrical aspect of the beam (which is related to the existence of the orbital angular momentum) could not be proved. Therefore a beam characterization that uses no cylindrical lenses is not enough, as was shown theoretically in Ref. 8.

With the above result in mind, we show how to complete a full ten second-order-moments characterization of a laser beam (from these moments the physical parameters could also be determined, as was shown in Ref. 12). For this purpose, we use a transversely excited atmospheric (TEA) CO_2 laser that delivers a doughnut beam. We used this laser in a number of previous studies.[13–16] Its doughnut-shaped profile suggests that the beam could carry orbital angular momentum, although previously we had no direct proof of that. To complete this study, we start by summarizing the theory and the previous results in Section 2. Section 3 is devoted to the experimental setup and to a discussion of the results. Conclusions are given in Section 4.

2. THEORY AND PREVIOUS RESULTS

Let us consider a laser beam that is propagating in the z direction and is described by its Wigner distribution function $h(x, y, u, v)$, where x and y are the transversal coordinates and u and v represent angles in paraxial propagation. In a second-order characterization the laser

0740-3232/2001/071726-08$15.00

beam is represented by its beam matrix **P**, which is defined in terms of the second-order averages of $h(x, y, u, v)$.[1,3,5,9] The beam matrix **P** is a 4×4 real, symmetric, and positive definite matrix. It is composed of three 2×2 submatrices, **W, M**, and **U**, and has a maximum of ten independent elements[1,3,5,8–10,12]:

$$\mathbf{P} = \begin{bmatrix} \mathbf{W} & \mathbf{M} \\ \mathbf{M}^t & \mathbf{U} \end{bmatrix} = \begin{bmatrix} \langle x^2 \rangle & \langle xy \rangle & \langle xu \rangle & \langle xv \rangle \\ \langle xy \rangle & \langle y^2 \rangle & \langle yu \rangle & \langle yv \rangle \\ \langle xu \rangle & \langle yu \rangle & \langle u^2 \rangle & \langle uv \rangle \\ \langle xv \rangle & \langle yv \rangle & \langle uv \rangle & \langle v^2 \rangle \end{bmatrix}. \quad (1)$$

In matrix (1) $\mathbf{W} = \mathbf{W}^t$ represents the (squared) beam width, $\mathbf{U} = \mathbf{U}^t$ is the (squared) beam divergence, and **M** is a nonsymmetric mixed matrix. The symmetric part of $\mathbf{W}^{-1}\mathbf{M}$ is the beam curvature, and the antisymmetric part of **M** is related to the orbital angular momentum that is transported by the beam.[6,12] Because we can do just irradiance measurements, only the **W** submatrix can be measured directly.[10] But **P** is transformed by *ABCD* optical systems (lenses and free spaces, among others) by use of the *ABCD* law,[1,5,8] allowing us to use different optics to obtain all its elements.[10,11] It is also important to note that, when a beam is modified by (or is propagating through) an *ABCD* optical system, there are two independent combinations of its **P** beam-matrix elements that remain invariant. We can choose these invariant parameters (or the generalized beam-propagation parameters, as we call them) to be the following normalized quantities[5,8–10,12]:

$$M_{\mathrm{eff}}^4 = 4k^2 (\det \mathbf{P})^{1/2} \geqslant 1, \quad (2)$$

$$t = 2k^2 T = 2k^2 \mathrm{Tr}(\mathbf{WU} - \mathbf{M}^2) \geqslant 1. \quad (3)$$

Here $k = 2\pi/\lambda$ is the modulus of the wave vector and λ is the wavelength of the beam. Instead of t from expression (3), it is better to define and use the normalized invariant quantity a, called intrinsic astigmatism[10]

$$a = t - M_{\mathrm{eff}}^4. \quad (4)$$

Unlike t, a has a straightforward physical interpretation: it allows one to define two disjoint classes of beams—the intrinsic stigmatic beams ($a = 0$) and the intrinsic astigmatic beams ($a > 0$).[8–10] The intrinsic astigmatism can be used in combination with M_{eff}^4, as in Ref. 10, or with another normalized invariant quantity, a_M, called the maximum intrinsic astigmatism, that is directly related to M_{eff}^4 through[8,9,12]

$$a_M = \frac{1}{2}(M_{\mathrm{eff}}^4 - 1)^2. \quad (5)$$

We now have the following double inequality:

$$0 \leqslant a \leqslant a_M. \quad (6)$$

M_{eff}^4 is related to the extension of the beam in phase space, i.e., the closer M_{eff}^4 is to one, the smaller is the phase-space extent of the beam, approaching the phase-space extent of a TEM_{00} beam of the same wavelength. Because the beam matrix **P** changes when the beam propagates through *ABCD* optical systems whereas a and M_{eff}^4, or, alternatively, a and a_M, remain invariant, we consider the beam-propagation parameters to be even more important than **P** to the characterization of a beam. Four disjoint families of beams were defined on the basis of the four possible combinations of pairs of beam-propagation parameters: ($a = 0$, $a_M = 0$), ($a = 0$, $a_M > 0$), ($a > 0$; $a_M > 0$, $a < a_M$), and ($a = a_M > 0$, $a_M > 0$). Their physical meaning was given in Ref. 9.

A physical parameter that is useful for our purposes is the orbital angular momentum per photon l_z. This quantity can be obtained from the antisymmetric part of **M**: $m = (\langle xv \rangle - \langle yu \rangle)/2$. The time-averaged orbital angular-momentum flux $\bar{J}_z^L$ of a partially coherent beam through a z plane is given by[6]

$$\bar{J}_z^L = \frac{I}{c}(\langle xv \rangle - \langle yu \rangle), \quad (7)$$

where I is the beam power and c is the light speed. For such a beam the photon flux (photons per unit time) is $I/\hbar\omega$, with $\hbar$ and ω being the normalized Plank's constant and the angular frequency ($\omega = kc$), respectively. Finally, we obtain the orbital angular momentum per photon l_z:

$$l_z = \bar{J}_z^L \frac{\hbar\omega}{I} = k(\langle xv \rangle - \langle yu \rangle)\hbar = 2km\hbar. \quad (8)$$

We now consider the measurement procedure for obtaining the beam-matrix elements. A simple way to obtain the elements of **P** is to measure transversal profiles of the beam irradiance at different z planes with a camera. From those profiles $\langle x^2 \rangle_z$, $\langle xy \rangle_z$, and $\langle y^2 \rangle_z$ can be calculated. With a parabolic fit of those values, we can obtain most of the elements of **P** at $z = 0$ because in free-space propagation we have

$$\langle x^2 \rangle_z = \langle x^2 \rangle_0 + 2\langle xu \rangle_0 z + \langle u^2 \rangle z^2, \quad (9)$$

$$\langle xy \rangle_z = \langle xy \rangle_0 + (\langle xv \rangle_0 + \langle yu \rangle_0) z + \langle uv \rangle z^2, \quad (10)$$

$$\langle y^2 \rangle_z = \langle y^2 \rangle_0 + 2\langle yv \rangle_0 z + \langle v^2 \rangle z^2. \quad (11)$$

In Eqs. (9)–(11) the subindex 0 indicates values at $z = 0$ (note that the divergence terms are z invariant; hence they have no subindex). But with this procedure it is impossible to obtain all the terms. We can measure **W**, **U**, and the symmetric part of **M**, but $\langle xv \rangle$ and $\langle yu \rangle$ always appear as $(\langle xv \rangle + \langle yu \rangle)$, so we cannot recover the antisymmetric part of **M**. It can be proved that this coupling cannot be broken with spherical lenses either. That is why a second set of measurements that includes the use of at least one cylindrical lens is needed.[8,10,11]

The crossed term $\langle uv \rangle_L$ of the divergence submatrix $\mathbf{U}_L$ just after a cylindrical lens with a convergence $1/f_x'$ in the x direction can be expressed with respect to the beam-matrix elements just before the lens (with no subindex) by

$$\langle uv \rangle_L = \langle uv \rangle - \frac{\langle xv \rangle}{f_x'}. \quad (12)$$

In this way the antisymmetric part of **M**, $m = (\langle xv \rangle - \langle yu \rangle)/2$, can be recovered:

$$m = \tfrac{1}{2}(\langle xv\rangle - \langle yu\rangle)$$
$$= (\langle uv\rangle - \langle uv\rangle_L)f'_x - \tfrac{1}{2}(\langle xv\rangle + \langle yu\rangle). \quad (13)$$

Using Eq. (13), one can complete the ten-parameter characterization after the quantity $\langle uv\rangle_L$ is determined. This value can be obtained from a parabolic fit for the beam measured in free space after the cylindrical lens by use of a formula analogous to Eq. (10).

To complete a full second-order characterization of a laser beam according to the above theory, we used a pulsed TEA CO_2 laser. This laser was selected for two reasons: First, we had obtained several previous results for that laser (see Refs. 13–16), but they were only partial in terms of second-order characterization, i.e., no cylindrical lens was used in those previous studies for beam characterization. Second, under some circumstances the output laser beam irradiance profile has a doughnut shape. Therefore it is considered to be a serious candidate as a beam for which it is not enough that a characterization be done with only rotationally symmetric optics [as is recommended in ISO document 11146 (Ref. 7)], i.e., characterization without a cylindrical lens in which the antisymmetric part of **M** would be ignored. The TEA CO_2 laser considered is a pulsed laser. It is important to note that the second-order-characterization formalism can be extended to pulsed beams under very general conditions.[16]

3. MEASUREMENTS AND DISCUSSION

The CO_2 laser is shown schematically in Fig. 1. It has a stable, half-symmetric resonator with a spherical mirror (radius of curvature of 10 m) and a flat output mirror. The cavity length is 1120 mm. Inside the resonator there is a Brewster plate for generating a linearly polarized beam and a circular diaphragm close to the curved mirror. The intracavity diaphragm controls the transverse modes, and it is essential for our measurements (we used diameters of 8, 10, and 11 mm for this circular diaphragm, as is explained below). Spherical lenses L_1 ($f'_1 = 254$ mm), L_2 ($f'_2 = 127$ mm), and L_3 ($f'_3 = 508$ mm) were used to condition the beam. The laser beam at $\lambda = 10.6\,\mu$m is pulsed and has an energy per pulse of $\simeq$0.5 J. The pulse structure contains an $\simeq$70-ns gain-switch peak that is followed by an $\simeq$2-μs tail. An electro-optical chopper selects a temporal slice inside the laser pulse. For reasons that are explained below, in our experiments, we used a thick time slice ($\Delta t_0 = 100$ ns) in the tail region of the pulse (500 ns after the beginning of the pulse, $t_0 > 500$ ns). To measure the elements of the beam matrix **P**, we took transversal profiles of the beam

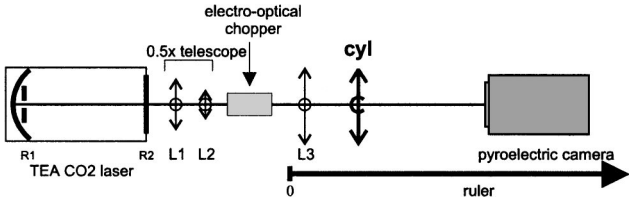

Fig. 1. The cylindrical lens (cyl) is used to decouple the $\langle xv\rangle + \langle yu\rangle$ term.

irradiance by using a pyroelectric camera (Spiricon, Model Pyrocam I). The cylindrical lens ($f'_x = 184$ mm) was used to put in evidence the antisymmetric part of the submatrix **M**, as was explained in Section 2.

Now we briefly explain the measurements that were done previously and the results that were obtained by use of the three values of the circular diaphragm before we describe the full beam characterization. For the 8-mm diaphragm, a rounded Gaussian-like beam is obtained in free space (M^2 close to 1), and its behavior is nearly constant along the pulse.[14] With the 10-mm diaphragm the output beam has a significant doughnut-shaped contribution and remains rotationally symmetric in free-space propagation. For that beam, we measured the output profiles, performed mode-beating measurements, and carried out a second-order characterization by using rotationally symmetric optics.[15] From those measurements, we know that, at the leading edge of the pulse (from the beginning of the pulse to $t_0 \simeq 100$ ns), there is only one mode. After that, there is a transition region, and, finally, the beam reaches a doughnutlike spatial structure with two modes ($t_0 > 500$ ns), although the central minimum is not zero.

For the 11-mm diaphragm preliminary results showed highly similar behavior for the $t_0 > 500$-ns region. From the mode-beating measurements, we also found two transversal modes, but the irradiance profile was closer to a purely doughnut-shaped spatial structure with a nearly zero irradiance at the central minimum. Because of these characteristics, the 11-mm diaphragm was used in the measurements considered in this paper, and the second-order-moments characterization was done for a thick time slice ($\Delta t_0 = 100$ ns) in the tail region of the pulse ($t_0 > 500$ ns) that was produced with the 11-mm intracavity diaphragm.

We now describe the actual measurements done in this experiment. To check the setup, we took a first set of measurements by using the 8-mm diaphragm. We do not expect the Gaussian-like beam with M^2 close to one[14] to have any general astigmatism or angular momentum. This beam was used to check the orientation of the cylindrical lens. Measurements of this beam were done without and with the cylindrical lens.

Typical beam profiles obtained with the 8-mm diaphragm are shown in Figs. 2(a) and 2(b). In both cases the laser output profile was very reproducible from shot to shot. Figure 2(c) shows the second-order moments that characterized the (squared) beam size. With no cylindrical lens, beam profiles were taken from $z = 350$ mm to $z = 1350$ mm, but those taken after $z = 600$ mm were hidden to simplify the figure. One can see that, before the cylindrical lens, the beam is rotationally symmetric. After the lens, the beam remains Gaussian like, but it is deformed along the x axis, as is expected. The cylindrical lens acts on $\langle x^2\rangle$, leaving $\langle y^2\rangle$ unaffected. At the same time the $\langle xy\rangle$ parabola after the lens is close to zero and is nearly flat, so we find that the output beam does not rotate (or that its total rotation is negligible), as is shown in the lower part of Fig. 2(c). As expected, from a stigmatic input beam, before the cylindrical lens an aligned simple astigmatic beam is obtained after a cylindrical lens with power along the x axis.

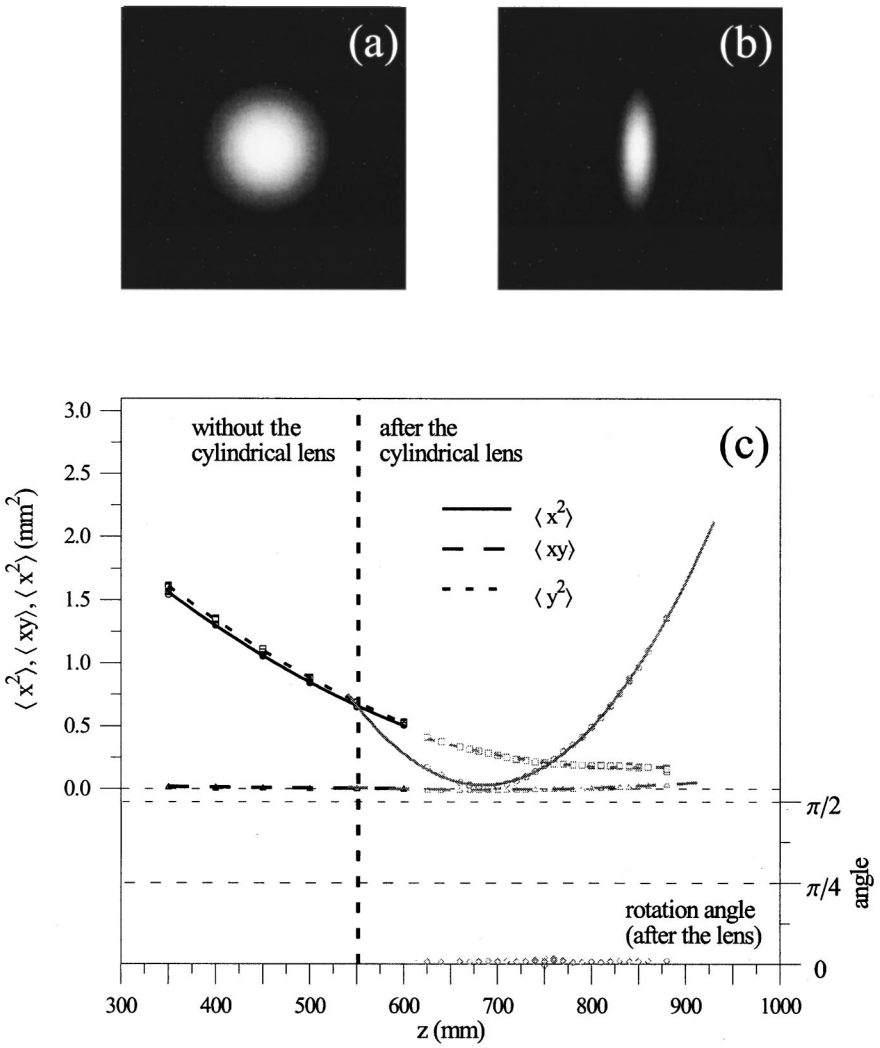

Fig. 2. Typical beam profiles obtained with the 8-mm diaphragm (a) with no cylindrical lens and (b) after the cylindrical lens, both taken at $z = 650$ mm. (c) Experimental values of $\langle x^2 \rangle$, $\langle xy \rangle$, and $\langle y^2 \rangle$ obtained before and after the cylindrical lens with the 8-mm diaphragm. Before the lens the beam is rotationally symmetric, and after the lens the beam is a simple astigmatic beam aligned along the lens axes. Note that the rotation angle is negligible.

After checking the setup with the Gaussian-like beam that was produced by the 8-mm diaphragm, we started the characterization of the doughnut-shaped beam that was produced with the 11-mm diaphragm. A first group of measurements was taken without the cylindrical lens. It is important to note that, with no cylindrical lens, the laser output profile is quite reproducible from shot to shot. A rotationally symmetric beam with a profile similar to the one shown in Fig. 3(a) is always obtained. From those irradiance profiles, we measured the following coefficients for Eqs. (9)–(11):

$$\langle x^2 \rangle = (5.08 \pm 0.02) - [(12.04 \pm 0.04) \times 10^{-3}]z + [(7.69 \pm 0.03) \times 10^{-6}]z^2, \quad (14)$$

$$\langle xy \rangle = (51 \pm 5) \times 10^{-3} - [(90 \pm 20) \times 10^{-6}]z + [(47 \pm 9) \times 10^{-9}]z^2, \quad (15)$$

$$\langle y^2 \rangle = (5.37 \pm 0.01) - [(12.64 \pm 0.04) \times 10^{-3}]z + [(7.97 \pm 0.02) \times 10^{-6}]z^2. \quad (16)$$

In Eqs. (14)–(16), the units for z are millimeters, and those for $\langle x^2 \rangle$, $\langle xy \rangle$, and $\langle y^2 \rangle$ are millimeters squared. The error factors included in those formulas are due to the parabolic fitting of the experimental data. Crossed terms in the errors of each parabola are not written but were considered in the calculations that follow. The experimental results and the parabolic fits can be seen on the left-hand side of Fig. 3(c) in which measurements with no cylindrical lens after $z = 600$ mm were suppressed for the sake of clarity. The results were remarkably reproducible.

For the second set of measurements a cylindrical lens was used. For this type of beam at least two kinds of behavior are possible after the cylindrical lens: A doughnut-shaped beam can be obtained by the addition of the irradiances of a TEM_{01} and a TEM_{10} Hermite–Gauss mode. We can call that type of beam an irradiance doughnut. Another way to obtain a doughnut-shaped beam is to add those two modes but in a coherent way (i.e., to add their electric fields) with $+\pi$ or $-\pi$ phases. In such a case, we would have a Laguerre–Gauss beam:

LG_0^{+1} or LG_0^{-1}. We can call them amplitude doughnuts. The difference between these two types of doughnut-shaped beams can be seen by the propagation of the beams through a cylindrical lens. An irradiance doughnut indicates a stigmatic beam and therefore an intrinsic stigmatic beam,[9] and its propagation through a cylindrical lens merely makes the doughnut elliptical (it flattens the irradiance profile), imposing on it the symmetry axes of the cylindrical lens. The beam is still intrinsic stigmatic after the lens, but it has an aligned simple astigmatic symmetry. On the other hand, an amplitude doughnut indicates an intrinsic astigmatic beam of the pseudostigmatic type,[8,9] and propagation through a cylindrical lens maintains its intrinsic astigmatism but destroys the pseudosymmetry of the beam; the beam becomes a rotating general astigmatic beam.[9] In the case of a $LG_0^{\pm 1}$ beam the beam is divided into two lobes.

For these measurements the cylindrical lens was placed at $z_L = 565$ mm. A typical beam profile after the cylindrical lens is shown in Fig. 3(b). But, in contrast with the high reproducibility of the output beam profile and the corresponding measurements made without the cylindrical lens, in this case, we found that the laser pattern could change from shot to shot. This fact is reflected in Fig. 4. For most pulses [approximately 75% of them, Fig. 4(a)] the beam profiles are rotated clockwise, and in only a few cases [approximately 5%, Fig. 4(c)] they are rotated counterclockwise. These are original intrinsic astigmatic beams from the laser that had a pseudostigmatic (rotational) symmetry in free space [the round irradiance profile of Fig. 3(a)] before the cylindrical lens. In some other cases [approximately 20%, Fig. 4(b)] the beam profile is elliptical (flattened), indicating a true stigmatic beam before the cylindrical lens and an aligned simple astigmatic one after the cylindrical lens.[9] Note that pulsed laser beams that seem to be fully reproducible when we consider only rotationally symmetric optics (suggesting only truly stigmatic beams) are not as simple as they appear at first sight. Also note that, for most pulses, the beam is of the intrinsic astigmatic, pseudostigmatic type.

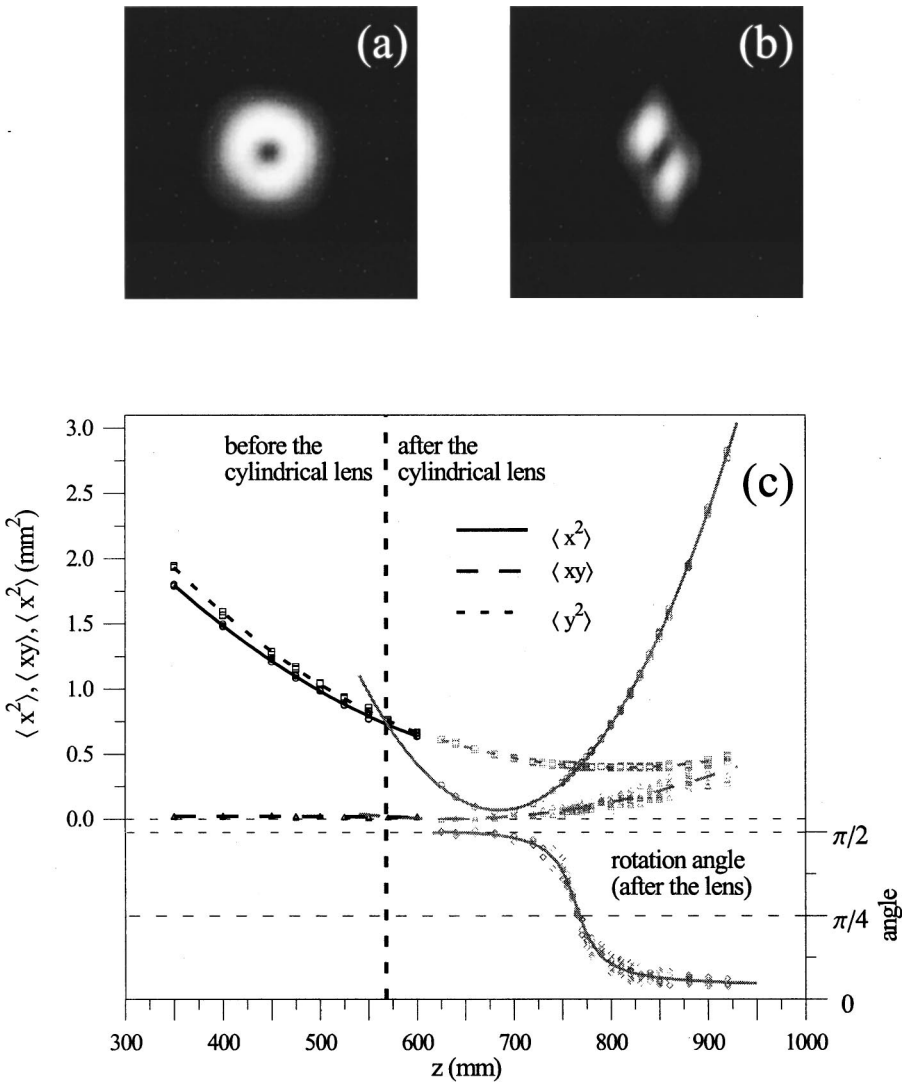

Fig. 3. Typical beam profiles obtained with the 11-mm diaphragm (a) with no cylindrical lens and (b) after the cylindrical lens, both taken at $z = 725$ mm. (c) Experimental values of $\langle x^2 \rangle$, $\langle xy \rangle$, and $\langle y^2 \rangle$ obtained before and after the cylindrical lens with the 11-mm diaphragm. Only pulses that rotate clockwise were considered after the lens. Before the lens the beam is rotationally symmetric, but after the lens the beam profiles rotate as shown.

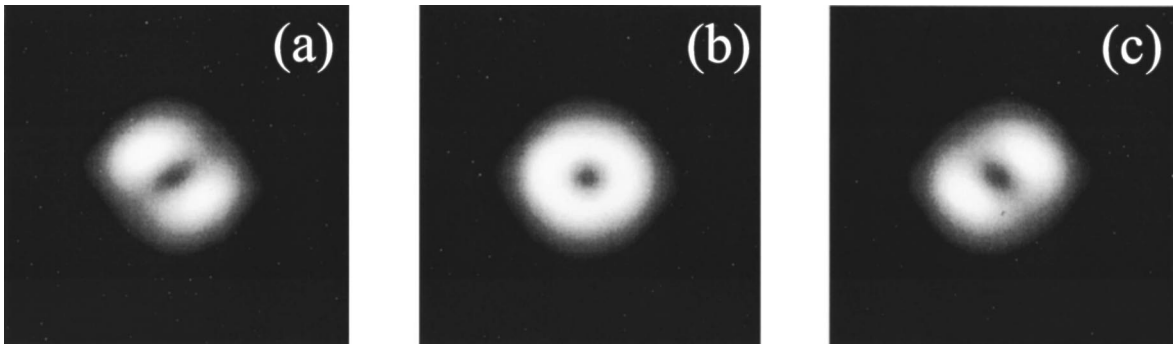

Fig. 4. Beam profiles taken at $z = 775$ mm after the cylindrical lens: (a) clockwise rotated (75% of the pulses), (b) aligned elliptical (flattened) profile (20% of the pulses), (c) counterclockwise rotated (5% of the pulses).

To explain the existence of the three types of beams emitted by our laser, we have to consider that in TEA CO_2 lasers usually there is more than one longitudinal mode. In our case the laser emits approximately 20 longitudinal modes. The intracavity diaphragm selects the transversal modes, but the longitudinal modes are mutually independent; thus some of them could rotate clockwise, whereas others rotate counterclockwise. If nearly all the modes rotate clockwise, we obtain a beam such as that shown in Fig. 3(b) or Fig. 4(a), whereas if most of them rotate counterclockwise something similar to that shown in Fig. 4(c) is measured. Intermediate behaviors appear between those two pure cases. The predominance of clockwise-rotating beams could be explained by a small asymmetry inside the laser cavity.

We completed the second-order-moments characterization for the clockwise-rotating beams [those shown in Figs. 3(b) and 4(a)]. The $\langle x^2\rangle$, $\langle xy\rangle$, and $\langle y^2\rangle$ values for those beams together with the parabolic fits are shown on the right-hand side of Fig. 3(c). The rotation angle for those profiles is also shown in the figure. From the experimental values, we obtained the following free-propagation parabolae:

$$\langle x^2\rangle_L = (23.3 \pm 0.1) - [(67.8 \pm 0.3) \times 10^{-3}]z + [(49.5 \pm 0.2) \times 10^{-6}]z^2, \quad (17)$$

$$\langle xy\rangle_L = (1.8 \pm 0.3) - [(5.7 \pm 0.7) \times 10^{-3}]z + [(4.5 \pm 0.5) \times 10^{-6}]z^2, \quad (18)$$

$$\langle y^2\rangle_L = (4.51 \pm 0.07) - [(10.2 \pm 0.2) \times 10^{-3}]z + [(6.2 \pm 0.1) \times 10^{-6}]z^2, \quad (19)$$

with z in millimeters and $\langle x^2\rangle_L$, $\langle xy\rangle_L$, and $\langle y^2\rangle_L$ in units of millimeters squared.

Equations (14)–(16) and (17)–(19) contain all the information that we need to complete the characterization (only the crossed terms in the error arising from the parabolic fit were not explicitly written). From Eqs. (14)–(16), we have for the initial beam at $z = z_L$

$$\mathbf{W}^{z_L} = \begin{bmatrix} (730 \pm 10) \times 10^{-3} & (14.6 \pm 0.7) \times 10^{-3} \\ (14.6 \pm 0.7) \times 10^{-3} & (770 \pm 10) \times 10^{-3} \end{bmatrix}, \quad (20)$$

$$\mathbf{M}^{z_L} = \begin{bmatrix} -(1.66 \pm 0.02) \times 10^{-3} & -(19 \pm 2) \times 10^{-6} + m \\ -(19 \pm 2) \times 10^{-6} - m & -(1.80 \times 0.03) \times 10^{-3} \end{bmatrix}, \quad (21)$$

$$\mathbf{U}^{z_L} = \begin{bmatrix} (7.69 \pm 0.03) \times 10^{-6} & (47 \pm 9) \times 10^{-9} \\ (47 \pm 9) \times 10^{-9} & (7.97 \pm 0.02) \times 10^{-6} \end{bmatrix}, \quad (22)$$

where m is the antisymmetric part of the $\mathbf{M}^{z_L}$ submatrix. In a similar way, from Eqs. (17)–(19) at $z = z_L$, we have

$$\mathbf{W}_L^{z_L} = \begin{bmatrix} (760 \pm 40) \times 10^{-3} & (20 \pm 20) \times 10^{-3} \\ (20 \pm 20) \times 10^{-3} & (770 \pm 10) \times 10^{-3} \end{bmatrix}, \quad (23)$$

$$\mathbf{M}_L^{z_L} = \begin{bmatrix} -(5.83 \pm 0.2) \times 10^{-3} & -(300 \pm 100) \times 10^{-6} + m_L \\ -(300 \pm 100) \times 10^{-6} - m_L & -(1.53 \pm 0.03) \times 10^{-3} \end{bmatrix}, \quad (24)$$

$$\mathbf{U}_L^{z_L} = \begin{bmatrix} (49.5 \pm 0.2) \times 10^{-6} & (4.5 \pm 0.5) \times 10^{-6} \\ (4.5 \pm 0.5) \times 10^{-6} & (6.2 \pm 0.1) \times 10^{-6} \end{bmatrix}, \quad (25)$$

for the beam after the cylindrical lens with m_L being the antisymmetric part of $\mathbf{M}_L^{z_L}$. Finally, by using Eq. (13), we find

$$m = -(810 \pm 90) \times 10^{-6}\,\text{mm}. \quad (26)$$

With this value, we have completed the measurement of all the elements in $\mathbf{P}^{z_L}$ for the clockwise-rotating beams.

We return now to calculate the beam-propagation parameters and the orbital angular momentum that is carried by some of the above-measured beams. If we had ignored the intrinsic astigmatism of the beam by not using the cylindrical lens in the measurement and thus setting $m = 0$, we would have had

$$M^4_{\mathrm{eff}} = 4.03 \pm 0.01, \tag{27}$$

$$t = 4.03 \pm 0.01, \tag{28}$$

$$a = (2.0 \pm 0.2) \times 10^{-3}, \tag{29}$$

$$a_M = 4.58 \pm 0.03 \tag{30}$$

and no orbital angular momentum

$$l_z = 0. \tag{31}$$

With the numbers from Eqs. (27)–(31), we would have considered that we had almost an intrinsic stigmatic beam ($a \simeq 0$). But with the full characterization the result is quite different:

$$M^4_{\mathrm{eff}} = 3.1 \pm 0.2, \tag{32}$$

$$t = 5.0 \pm 0.2, \tag{33}$$

$$a = 1.8 \pm 0.4, \tag{34}$$

$$a_M = 2.2 \pm 0.4, \tag{35}$$

$$l_z = -(1.0 \pm 0.1)\hbar. \tag{36}$$

Now we know that we have an intrinsic astigmatic beam belonging to the third of the four disjoint families of beams mentioned in Section 2, $a > 0$ and $a < a_M$, and in its initial form the beam transports orbital angular momentum, $l_z \neq 0$. Note that, in Eqs. (27)–(36), we consider only the errors derived from the fitting of the experimental data to Eqs. (9)–(11).

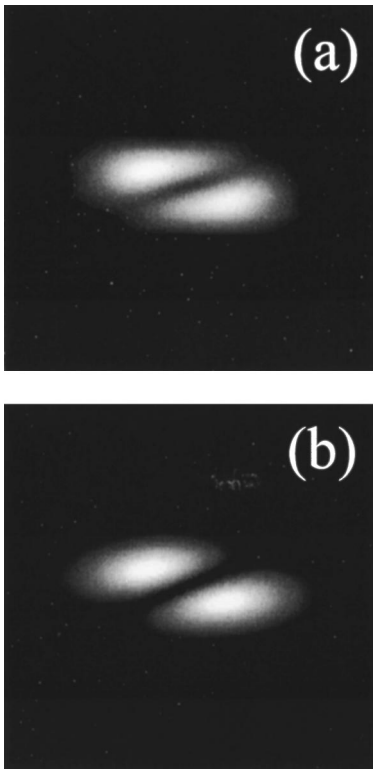

Fig. 5. Beam irradiance profiles at $z = 920$ mm (after the cylindrical lens): (a) an actual experimental profile, (b) a pure (theoretical) LG_0^{-1} beam.

From the irradiance profiles, we also know the general shape of the beam. It is a doughnut-shaped beam, so it would be interesting to compare our results with those of a LG beam. We could compare the experimental irradiance profiles with those obtained from a numerical propagation of a LG_0^{-1} beam. As one can see from Fig. 5, for a z plane situated after the lens the results are very similar. It could also be interesting to calculate the invariant parameters and l_z for a LG_0^{-1} beam. For such a beam the result is

$$M^4_{\mathrm{eff}} = 3, \tag{37}$$

$$t = 5, \tag{38}$$

$$a = 2, \tag{39}$$

$$a_M = 2, \tag{40}$$

$$l_z = -\hbar. \tag{41}$$

These values are close to the experimental ones [Eqs. (32)–(36)]. We could say that the clockwise-rotating pulses contain nearly pure LG_0^{-1} modes.

4. SUMMARY AND CONCLUSIONS

From the theory and the experiments presented in this paper, one can see that a cylindrical lens is needed to complete a full second-order-moments characterization of a laser beam, including the measurement of the angular momentum transported by the beam. A characterization without such a lens would lead us to incomplete or even erroneous conclusions, as was explained in Ref. 8. But even if we were not interested in a full second-order characterization, a cylindrical lens could show us features of the beam that remain hidden if only rotationally symmetric optical systems are considered. We have seen that our laser had this type of behavior. Its beam profile seemed to be very reproducible in free space without the cylindrical lens; only after the cylindrical lens, as is shown in Fig. 4, was the fact revealed that the laser emitted different kinds of beam profiles. The cylindrical lens also allowed us to complete a second-order characterization of our beam in the case of pulses that display a clockwise-rotating transverse irradiance pattern. We have seen that those pulses consist of nearly pure LG_0^{-1} modes and transport an orbital angular momentum of $l_z \simeq -\hbar$ per photon.

ACKNOWLEDGMENTS

This research was supported by the Comisión Interministerial de Ciencia y Tecnología of Spain under project PB97-0295.

J. Serna, the corresponding author, can be reached at the address on the title page or by e-mail, fiopt01@sis.ucm.es. G. Nemeş's e-mail address is gnemes98@hotmail.com.

REFERENCES

1. M. J. Bastiaans, "Wigner distribution function and its application to first-order optics," J. Opt. Soc. Am. **69**, 1710–1716 (1979).
2. S. Lavi, R. Prochaska, and E. Keren, "Generalized beam parameters and transformation laws for partially coherent light," Appl. Opt. **27**, 3696–3703 (1988).
3. R. Simon, N. Mukunda, and E. C. G. Sudarshan, "Partially coherent beams and a generalized *ABCD*-law," Opt. Commun. **65**, 322–328 (1988).
4. A. E. Siegman, "New developments in laser resonators," in *Laser Resonators*, D. A. Holmes, ed., Proc. SPIE **1224**, 2–14 (1990).
5. J. Serna, R. Martínez-Herrero, and P. M. Mejías, "Parametric characterization of general partially coherent beams propagating through *ABCD* optical systems," J. Opt. Soc. Am. A **8**, 1094–1098 (1991).
6. J. Serna and J. M. Movilla, "Orbital angular momentum of partially coherent beams," Opt. Lett. **26**, 405–407 (2001).
7. International Organization for Standardization, Technical Committee/Subcommittee 172/SC9, "Lasers and laser-related equipment—test methods for laser beam parameters—beam widths, divergence angle and beam propagation factor," ISO doc. 11146: 1999 (International Organization for Standardization, Geneva, Switzerland, 1999).
8. G. Nemeş and J. Serna, "Do not use spherical lenses and free spaces to characterize beams: a possible improvement of the ISO/DIS 11146 document," in *Proceedings of the Fourth Workshop on Laser Beam and Optics Characterization*, A. Giesen and M. Morin, eds. (Verein Deutscher Ingenieure-Technologiezentrum, Düsseldorf, Germany, 1997), pp. 29–49.
9. G. Nemeş and J. Serna, "Laser beam characterization with use of second order moments: an overview," in *DPSS Lasers: Applications and Issues*, M. W. Dowley, ed., Vol. 17 of OSA Trends in Optics and Photonics Series (Optical Society of America, Washington, D.C., 1998), pp. 200–207.
10. G. Nemeş and A. E. Siegman, "Measurement of all ten second-order moments of an astigmatic beam by use of rotating simple astigmatic (anamorphic) optics," J. Opt. Soc. Am. A **11**, 2257–2264 (1994).
11. B. Eppich, C. Gao, and H. Weber, "Determination of the ten second order intensity moments," Opt. Laser Technol. **30**, 337–340 (1998).
12. G. Nemeş and J. Serna, "The ten physical parameters associated with a full general astigmatic beam: a Gauss Schell-model," in *Proceedings of the Fourth Workshop on Laser Beam and Optics Characterization*, A. Giesen and M. Morin, eds. (Verein Deutscher Ingenieure-Technologiezentrum, Düsseldorf, Germany, 1997), pp. 92–105.
13. C. Martínez, F. Encinas-Sanz, J. Serna, P. M. Mejías, and R. Martínez-Herrero, "On the parametric characterization of the transversal spatial structure of laser pulses," Opt. Commun. **139**, 299–305 (1997).
14. F. Encinas-Sanz, J. Serna, C. Martínez, R. Martínez-Herrero, and P. M. Mejíias, "Time-varying beam quality factor and mode evolution in TEA CO_2 laser pulses," IEEE J. Quantum Electron. **34**, 1835–1838 (1998).
15. C. Martínez, J. Serna, F. Encinas-Sanz, R. Martínez-Herrero, and P. M. Mejías, "Time-resolved spatial structure of TEA CO_2 laser pulses," Opt. Quantum Electron. **32**, 17–30 (2000).
16. P. M. Mejías and R. Martínez-Herrero, "Time-resolved spatial parametric characterization of pulsed light beams," Opt. Lett. **20**, 660–662 (1995).